Julia Ott, Jessica Sehr, Nadine Schmidt, Wolfgang Schliebs and Ralf Erdmann*

Comparison of human PEX knockout cell lines suggests a dual role of PEX1 in peroxisome biogenesis

https://doi.org/10.1515/hsz-2022-0223
Received July 7, 2022; accepted December 5, 2022;
published online December 19, 2022

Abstract: For the biogenesis and maintenance of peroxisomes several proteins, called peroxins, are essential. Malfunctions of these proteins lead to severe diseases summarized as peroxisome biogenesis disorders. The different genetic background of patient-derived cell lines and the residual expression of mutated PEX genes impede analysis of the whole spectrum of cellular functions of affected peroxins. To overcome these difficulties, we have generated a selected PEX knockout resource of HEK T-REx293 cells using the CRISPR/Cas9 technique. Comparative analyses of whole cell lysates revealed PEX-KO specific alterations in the steady-state level of peroxins and variations in the import efficacy of matrix proteins with a Type 2 peroxisomal targeting signal. One of the observed differences concerned PEX1 as in the complete absence of the protein, the number of peroxisomal ghosts is significantly increased. Upon expression of PEX1, import competence and abundance of peroxisomes was adjusted to the level of normal HEK cells. In contrast, expression of an alternatively spliced PEX1 isoform lacking 321 amino acids of the N-terminal region failed to rescue the peroxisomal import defects but reduced the number of peroxisomal vesicles. All in all, the data suggest a novel 'moonlighting' function of human PEX1 in the regulation of pre-peroxisomal vesicles.

Keywords: CRISPR/Cas9; moonlighting functions; peroxins; peroxisome; PEX1.

***Corresponding author: Ralf Erdmann**, Department of Systems Biochemistry, Institut für Biochemie und Pathobiochemie, Ruhr-Universität-Bochum, Systembiochemie, Gebäude MA, Postfach 26, Universitätsstr. 150, D-44801 Bochum, Germany, E-mail: ralf.erdmann@rub.de. https://orcid.org/0000-0001-8380-0342

Julia Ott, Jessica Sehr, Nadine Schmidt and Wolfgang Schliebs, Department of Systems Biochemistry, Institute for Biochemistry and Pathobiochemistry, Ruhr University Bochum, D-44780 Bochum, Germany. https://orcid.org/0000-0003-2762-3403 (W. Schliebs)

Introduction

The first peroxisomal biogenesis defect was described in 1964 by Bowen et al., who observed a characteristic set of symptoms from a group of children (Bowen et al. 1964). Diseases with corresponding symptoms, including a typical craniofacial dimorphism, severe cerebric aberrations as well as hepatic dysfunctions, were summarized as Zellweger syndrome (ZS). Later it became clear that these diseases are caused by a defect in the biogenesis of peroxisomes as these organelles appeared to be absent in ZS-patient derived cells (Goldfischer et al. 1973). The analysis of fibroblast cell lines from peroxisome biogenesis disorder (PBD) patients led to the identification of the responsible genes, which encode 14 so called PEX-proteins or peroxins (Moser et al. 1995; Suzuki et al. 2001). Peroxins are required for the biogenesis and maintenance of peroxisomes, including the import of membrane and matrix proteins as well as the division and inheritance of peroxisomes. PEX3 and PEX19 together with PEX16, which is missing in several lower eukaryotes, are responsible for the formation of peroxisomal membranes and the import of membrane proteins (Sacksteder et al. 2000; Shimozawa et al. 2000; Smith and Aitchison 2013; South and Gould 1999). Most of the matrix proteins are bound in the cytosol by the two import receptors PEX5 and PEX7 (Subramani 1998), either at a C-terminal peroxisomal targeting signal 1 (PTS1) (Gould et al. 1989) or at the PTS2-sequence located near the N-Terminus (Osumi et al. 1991), respectively. While PEX5 by its own acts as a receptor that cycles between the cytosol and peroxisomal membranes, PEX7 requires species-specific co-receptors. In human cells, this is taken over by a longer splice variant of PEX5, which contains a PEX7-binding site and is referred to as PEX5L (Otera et al. 2000). After cargo recognition, the PEX5-cargo complex binds to the docking proteins PEX14 and PEX13 at the peroxisomal membrane (Fransen et al. 1998; Gould et al. 1996). Several lines of evidence suggest that a transient pore is formed, through which the cargo could be translocated into the peroxisomal matrix (Meinecke et al. 2010). After cargo release, PEX5 is mono-ubiquitinated at a conserved cysteine residue by the RING-(really interesting new gene)-finger complex consisting of PEX2, PEX10 and

PEX12 (Miyata and Fujiki 2005) and extracted out of the peroxisomal membrane by the export complex, which is formed by the AAA$^+$-ATPases PEX1 and PEX6 and their membrane anchor PEX26 (Matsumoto et al. 2003, 2001; Portsteffen et al. 1997). After removement of the ubiquitin-moiety by cytosolic deubiquitinating enzymes (DUBs), PEX5 can fulfill another import cycle (Grou et al. 2012). Peroxisomal defects often lead to the formation of so called 'ghosts', which originally were defined as empty peroxisomal membrane structures of larger size when compared with mature peroxisomes (Santos et al. 1988). These peroxisomal structures are typical for fibroblast cells derived from Zellweger patients with peroxisomal matrix import defects.

The accumulation of fibroblast cell lines from many different PBD-patients led to the identification of several mutations among peroxins causing peroxisomal biogenesis disorders (Ebberink et al. 2011). For many years patient-derived fibroblast cell lines have been the only way to analyze the effects of peroxin mutations on the biogenesis and metabolism of peroxisomes (Ferdinandusse et al. 2016). However, there are several disadvantages connected to those patients-derived cell lines. First, in most of the cases there is no complete knockout of the respective peroxin, resulting in the expression of shortened or mutated versions of the proteins (Ebberink et al. 2011). Therefore, it is not possible to exclude residual activity, which would falsify the phenotype. Moreover, the heterogeneity of the diverse mutations and the different genetic background of the patient cell lines lead to an impeded comparability of the observed phenotypes (Slawecki et al. 1995). To overcome these challenges, we decided to establish PEX knockout cell lines that will enable the validation of the full spectrum of cellular functions of PEX genes either by phenotypic analyses or by expressing peroxin variants in a well-defined genetic background. To generate selected PEX-KO cell-lines, we used CRISPR/Cas9 technology (Doudna and Charpentier 2014) in otherwise isogenic HEK T-REx293 cells.

Phenotypic comparison of the isogenic PEX-KO cells disclosed peroxin-dependent effects on steady-state levels of peroxisomal proteins and differences in peroxisomal abundance, which had not been noted in Zellweger patient-derived cells. The PEX1 KO cell line exhibited the well-known import defect for peroxisomal matrix proteins but also an increased number of peroxisomal ghosts. Remarkably, the dysbalance in the number of ghosts was complemented by an alternatively spliced isoform of PEX1 that did not complement the import defect. The data show that the PEX-KO cell line collection is suitable for the comparable functional analysis of wild-type and mutant peroxins in an isogenic background, for a comparative analysis of the phenotypes caused by patient-derived mutant PEX-genes, and also for the investigation of moonlighting functions as well as alternative isoforms of peroxins.

Results

Generation of a PEX-KO cell line collection

For the generation of PEX-KO cell lines, we applied the CRISPR/Cas9 technique (Jinek et al. 2012). After designing specific RNAs that target the respective genes, we have used them to guide the Cas9 endonuclease, which then created a double strand break (DSB) at the desired location (Figure 1A). Because the repair of the DSB by non-homologous end-joining leads to different insertions or deletions (indels) on each allele, we amplified the respective gene area by PCR and after sequencing used the TIDE (tracking of indels by decomposition) software to determine mutations in mixed DNA samples (Brinkman et al. 2014). In parallel, we cloned and sequenced 20 individual DNA molecules to obtain the actual sequence of the shortened expression products (Figure 1A). Both methods allowed verification of the successful knockout.

Figure 1B shows a section of exon1 of the *PEX1* gene with the labelled guide sequence as an example. In case of the generation of the PEX1-KO, the TIDE-analysis revealed that the repair of the DSB led to the deletion of 7, 8 or 10 base pairs (Figure 1C). Since HEK293 cells, from which the HEK T-REx293 cell line derived, contain varying chromosome numbers (Binz et al. 2019), the analysis detected three alleles which have been repaired individually. Cloning and sequencing of 20 individual DNA molecules confirmed the result from the TIDE-analysis and revealed expression products of neglectable length (Figure 1D). Following this procedure, we generated nine selected PEX-KO cell lines, which include at least one member of every peroxin-group: PEX3, PEX16 and PEX19 (peroxisomal membrane formation), PEX5 and PEX7 (matrix protein import receptors), PEX13 and PEX14 (docking complex), PEX10 (RING-finger complex), PEX1 (export complex). Figure 1E shows the indel mutations of all generated KO cell lines, while the respective sequences of the remaining expression products are presented in Supplementary Table S1.

Expression of the respective peroxin leads to complementation of peroxisomal defects

Microscopic inspection of T-REx293 cells and the PEX-KO cells revealed a punctate pattern of the artificial peroxisomal

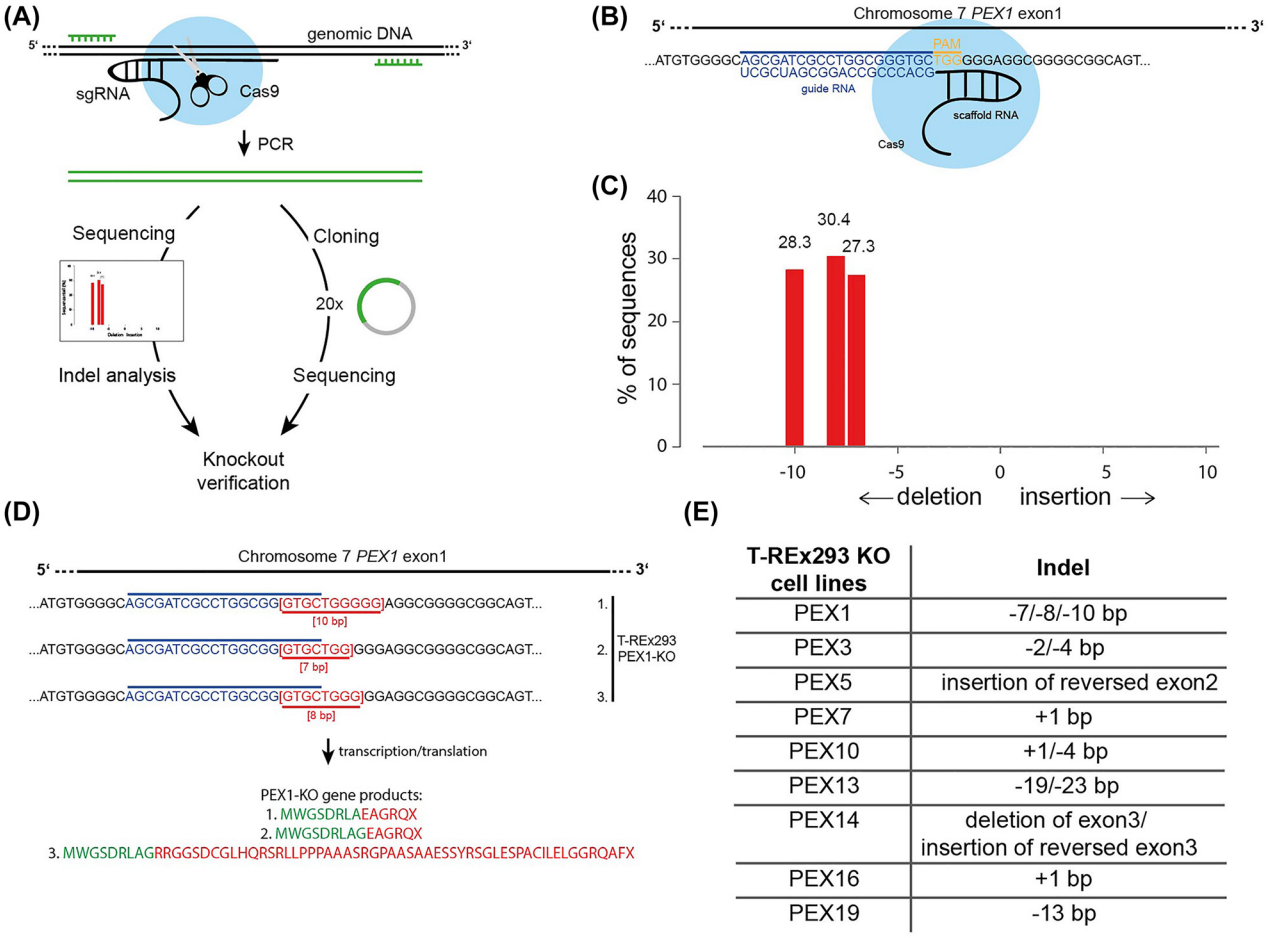

T-REx293 KO cell lines	Indel
PEX1	-7/-8/-10 bp
PEX3	-2/-4 bp
PEX5	insertion of reversed exon2
PEX7	+1 bp
PEX10	+1/-4 bp
PEX13	-19/-23 bp
PEX14	deletion of exon3/ insertion of reversed exon3
PEX16	+1 bp
PEX19	-13 bp

Figure 1: Procedure of creating a PEX-KO collection. (A) Chimeric single-guided RNAs (sgRNAs) were used to target the respective genes and guide the Cas9 endonuclease. Cas9 creates a double strand break (DSB), which is repaired by non-homologous end-joining. To identify the resulting insertions or deletions (indel) the respecting gene area was amplified by PCR and after sequencing a TIDE (tracking of indels by decomposition) analysis was performed, which determines indel mutations in mixed DNA-sequences. In parallel 20 single DNA-molecules were cloned and sequenced for knockout verification. (B) The chimeric RNA contains a 20-nucleotide sequence required for target DNA binding of Cas9 (guide RNA), while the other part of the chimeric RNA orientates the RNA in a proper secondary structure enhancing binding of Cas9 (scaffold RNA). The 20-nucleotide sequence is complementary to the area of the gene to be targeted, here exon1 of PEX1, and requires an adjacent GG dinucleotide-containing PAM sequence. (C) Indel spectrum of the PEX1-KO cell line determined by TIDE. The dissolution of the mixed DNA sequences showed that the repair of the DSB on every allele of exon1 of PEX1 led to the deletion of 7, 8 and 10 bp. The deletions occurred in similar frequencies (*y*-axis). (D) In case of PEX1, the repair of the DSB led to the deletion of 7, 8 and 10 base pairs (bp) on the respective alleles, which result in frame-shift mutations and significant shortening of the expression products. (E) Indel mutations of all generated PEX-KO cell lines. For some cell lines the repair of the DSB led to the indel of the same number of base pairs. PEX5-and PEX14-KO cell lines were generated by a different procedure leading to indels of whole exons (Galiani et al. 2022). Some chromosomes are present in three copies.

proteins EGFP-PTS1 (Figure 2A), whereas all generated KO cell lines except PEX7-KO exhibited an import defect for matrix proteins as indicated by the cytosolic mislocalization of the peroxisomal marker EGFP-PTS1 (Figure 2B). The PTS2-EGFP was used to test the PEX7-KO as PEX7 codes for the PTS2 receptor and its deficiency does only affect import of PTS2 proteins (Figure 2D, E), while deficiency in all other peroxins affects both import of both PTS1 and PTS2 protein. The observed mislocalization is typical for cell lines defective in peroxins of the peroxisomal import machineries and underlines the successful knock-out of the respective PEX genes. Cells with defective members of the membrane protein import machinery even lack detectable peroxisomal membranes, as indicated by the absence of the peroxisomal membrane marker PMP70 as seen for PEX3-KO (Figure 2B) or mislocalization of the peroxisomal membrane protein PEX14 to mitochondria as seen for PEX3-KO, PEX16-KO and PEX19-KO (data not shown). It has been identified that loss of peroxisomes leads to re-routing of several peroxisomal proteins, including PEX14 to mitochondria, which have been

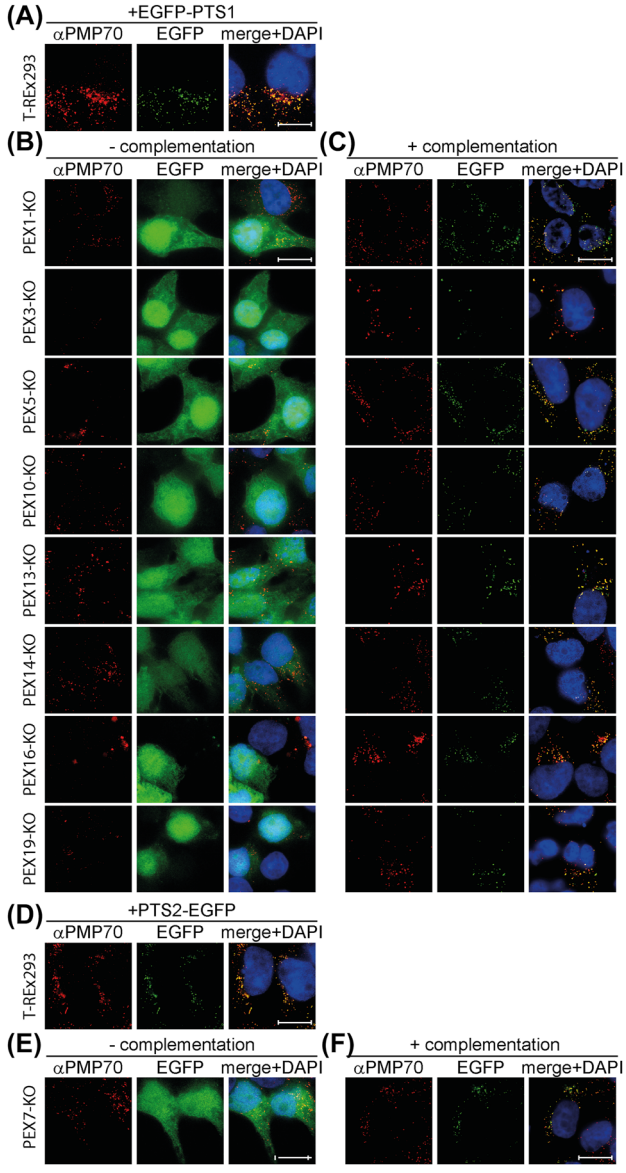

Figure 2: Peroxisomal defects in T-REx293 PEX-KO cell lines are complemented by transfection of the deleted PEX genes. Normal T-REx293 cells and PEX-KO cells were cultivated on coverslips and transfected with vectors encoding EGFP-PTS1 (A–C) or PTS2-EGFP (D–F) to monitor peroxisomal matrix protein import. In parallel, PEX-KO cell lines were transfected with vectors additionally coding for the corresponding deficient PEX gene to test for complementation of the PEX phenotype (C), (F). T-REx293, PEX1-, PEX5-, PEX7-, PEX10-, PEX13- and PEX14-KO cells were fixed 48 h and PEX3-, PEX16-, and PEX19-KO cells 96 h after transfection with formaldehyde. Peroxisomal membranes were labelled using *α*PMP70-antibodies, whereas nuclei were stained with DAPI. While the observed punctate pattern indicates the peroxisomal localization of the peroxisomal marker proteins EGFP-PTS1/PTS2-EGFP in T-REx293 cells, there is a cytosolic mislocalization of the marker proteins in PEX-KO cells. PEX3-KO cells even lack any detectable peroxisomal membranes as indicated by the absence of the marker PMP70. A fuzzy pattern in PEX19-KO cells indicates mislocalization or aggregation of the membrane marker PMP70. While most of the PEX16-KO cells are devoid of peroxisomal membranes, some cells exhibit enlarged import-competent peroxisomes. The plasmid-encoded expression of the respective peroxins led to the complementation of both membrane and matrix protein import defects. Scale bars: 10 µm.

described as places for emergency landing for abandoned peroxins (Nuebel et al. 2021). The fuzzy punctate pattern seen for PMP70 in PEX19-KO cells most likely represents mislocalization or aggregation of protein.

The PEX16-KO cells show an unusual heterogeneous phenotype. Most of the cells are defective in peroxisomal import of matrix and membrane proteins as indicated by the cytosolic mislocalization of the peroxisomal matrix marker and mislocalization or depletion of peroxisomal membrane proteins, as indicated by absence and aggregates of the membrane marker PMP70 (Figure 2B, Supplementary Figure S1) and mislocalization of PEX14 to mitochondria (data not shown). However, there is a subpopulation of PEX16-KO cells, which contain peroxisomal structures that are less in number and enlarged when compared with normal peroxisomes (Figure 2B, Supplementary Figure S1). Interestingly, there is a colocalization with EGFP-PTS1 (Supplementary Figure S1), indicating that these peroxisomal structures can import matrix proteins, as recently has been described for PEX16-KO HeLa cells (Yagita et al. 2022). This mosaic phenotype suggests that although PEX16 is important for peroxisomal membrane biogenesis, some mammalian cells remarkably can still form peroxisomes in its absence.

To show that the effect on peroxisome number and targeting is a result of the genetic manipulation, we examined whether the peroxisomal protein import defects can be complemented by the plasmid-encoded expression of the respective peroxin. For all KO cell lines the expression of the respective peroxins restored not only the import of matrix proteins, but also induced the formation of peroxisomal membranes in case they were absent (Figure 2C, F), as seen for PEX3-KO. After plasmid-encoded expression of PEX16 in PEX16-KO cells, the enlarged peroxisomal structures vanished and peroxisomes of normal size and number were formed.

PEX-KO cell lines differ in the steady-state level of peroxisomal proteins

The immunoblot analysis of whole cell lysates of the generated PEX-KO collection showed that the absence of some peroxins affect the steady-state levels of other peroxisomal proteins (Figure 3). The deletion of PEX1 for instance results

in a reduced PEX5 stability, which has already been observed in PEX1-deficient patient cell lines (Dodt and Gould 1996). The knockout of PEX14 also leads to an increased steady-state level of PEX13, while the absence of PEX5 destabilizes PEX14 as shown beforehand (Natsuyama et al. 2013). As new finding we observe that the deficiency in PEX1 also results in an increased PEX13 stability (Figure 3). To prove the significance of PEX13 stabilization in the absence of PEX1 we repeated immunoblot analyses of three independent clones (Supplementary Figure S2). Stabilization of PEX13 has been observed in *Hansenula polymorpha* upon deletion of PEX14 and RING-finger peroxins that seem to play a role in PEX13-degradation (Chen et al. 2018).

Moreover, some KO cell lines show partial import of the PTS2-protein thiolase (ACAA1), as indicated by the presence of maturated thiolase. As maturation of thiolase occurs after peroxisomal import and is caused by cleavage of the targeting signal, the presence of the mature forms suggests that these proteins have been transported into the peroxisomal lumen (Figure 3). This is especially the case for PEX10-KO cells, which show a nearly similar ratio of mature-and premature thiolase. The PEX7-KO cell line is the only cell line, which not only shows no maturated thiolase at all but an increased amount of accumulated premature thiolase that exceeds the total thiolase amount in control or other KO cell lines (Figure 3).

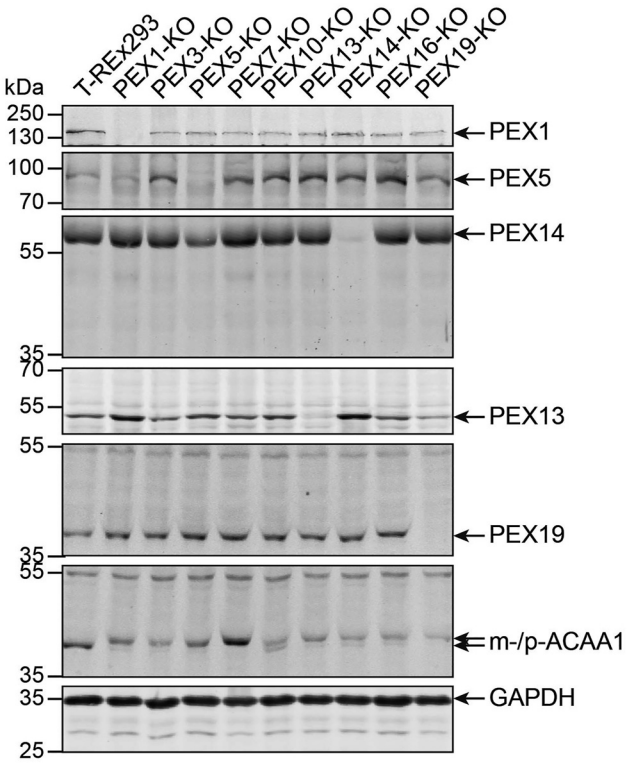

Figure 3: PEX-KO cell lines show differences in steady-state levels of peroxisomal proteins. Whole cell lysates of normal T-REx293 and PEX-KO cells were prepared and analyzed by immunoblotting using indicated antibodies. While a deletion of PEX1 leads to a decreased PEX5-and an increased PEX13-stability, an increased PEX13-stability is observed in PEX14-KO cells. Some KO cell lines, especially PEX10-KO show residual import of the PTS2-protein thiolase (ACAA1) as indicated by abundance of mature thiolase (m-ACAA1), which migrates faster than precursor thiolase (p-ACAA1) during electrophoresis due to peroxisomal cleavage of PTS2.

PEX1-KO cells exhibit an increased number of PMP70-containing peroxisomal vesicles

Immunofluorescence microscopy of PEX1-KO cells revealed that they contained increased numbers of PMP70-and PEX14-labelled peroxisomal structures that also appeared to be of reduced size when compared to peroxisomes in control cells (Figure 4A). The plasmid-encoded expression of PEX1 in PEX1-KO cells resulted in complementation of this phenotype, demonstrated by a reduction in peroxisome numbers and enlargement of peroxisomes, indistinguishable from those in control cells. We then took a closer look at the influence of the deletion of other peroxins on the number of PMP70-labelled structures. To this end, quantification of whole cell peroxisome numbers in ghost-containing KO-cells was performed (Figure 4B). Most of the deletion cell lines showed a similar number of peroxisomal ghosts as normal HEK T-REx293 cells, which contained about 250 peroxisomes per cell, while PEX1-KO cells in average exhibit nearly twice as many peroxisomal vesicles (Figure 4B). The only other KO cell line with significantly increased peroxisomal numbers is the PEX10-KO, albeit it did not reach numbers as high as observed for PEX1-KO cells (Figure 4B).

A splicing variant of PEX1 cannot rescue the import defect of PEX1-KO cells but restores peroxisome abundance

For several peroxins isoforms exist that have not yet been characterized in detail. Hence, we used the PEX1-KO cell line to investigate known isoforms of PEX1. Beside the full-length PEX1, there is a second alternatively spliced, short isoform, which lacks amino acids 92–413 (UniProtKB Identifier O43933-2) (Figure 5A). The deletion is expected to affect the N-terminal domain (NTD), which exhibits phospholipid-binding activity (Shiozawa et al. 2006). However, the deletion does not concern the two AAA^+-ATPase domains, which both are supposed to play critical roles for PEX1/PEX6 complex formation and extraction of the PTS1

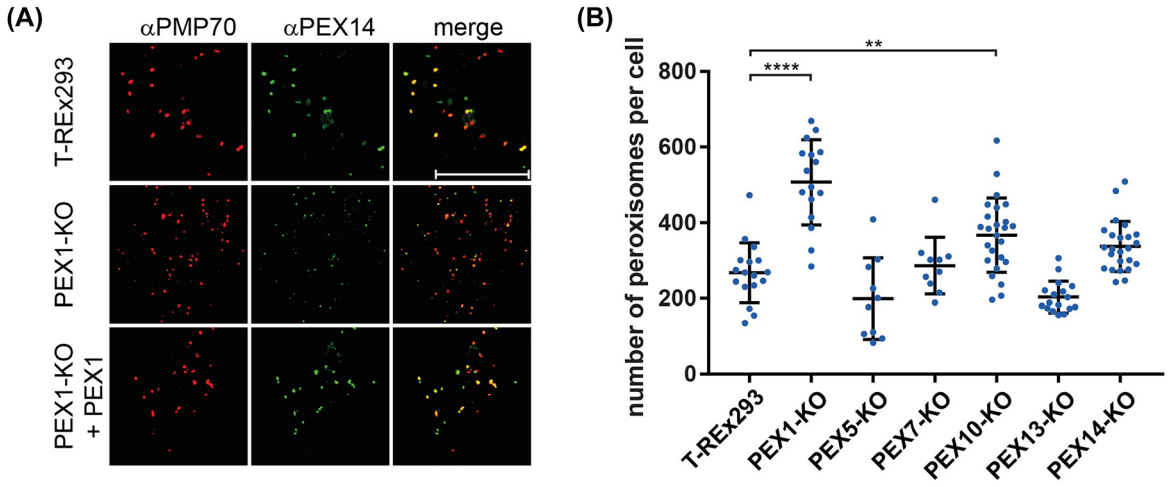

Figure 4: A deletion of PEX1 leads to an increased number of PMP70-labelled peroxisomal ghosts. (A) Representative fluorescence microscopy images of T-REx293 and PEX1-KO cells show that a deletion of PEX1 leads to a significantly increased number of PMP70-and PEX14-labelled peroxisomal ghosts, which appeared to be of decreased size. The expression of PEX1 restores peroxisomal size and number in PEX1-KO cells. Scale bar: 10 µm. (B) Peroxisomal number in T-REx293 and indicated KO cells was quantified from whole cell images after visualization of peroxisomal vesicles with *α*PMP70-antibodies using the spots function of IMARIS (BITPLANE Scientific Software). Data represent mean ± SD Peroxisomal number in PEX1-and PEX10-KO cells is significantly increased compared to T-Rex293 cells as analyzed by one-way ANOVA ($n \geq 2$, ****$p = 0.0001$, **$p = 0.0037$). Per replicate at least three cells were quantified for each cell line. Total number of cells analyzed: T-REx293, 17; PEX1-KO, 16; PEX5-KO, 10; PEX7-KO, 10; PEX10-KO, 25; PEX13-KO, 17; PEX14-KO, 24.

receptor from the membrane (Ciniawsky et al. 2015; Saffert et al. 2017). To study the cellular function of the short isoform, we expressed PEX1 as well as PEX1(Δ92-413) in PEX1-KO cells (Figure 5B) and compared their complementing activities. While reintroduction of PEX1 fully restores the peroxisomal import defect of matrix proteins (Figures 2C and 5C), cells expressing PEX1(Δ92-413) still show cytosolic mislocalization of EGFP-PTS1 (Figure 5C). This implies that not only the AAA$^+$-ATPase domains of PEX1 are essential for its role in receptor recycling, but also the N-terminal region.

The other prominent effect of a PEX1 deletion we have observed was the increased number of peroxisomal vesicles (Figure 4B). After expression of PEX1 in PEX1-KO cells the peroxisomal number was highly reduced and even reached T-REx293 levels (Figure 5D). Similarly, expression of PEX1(Δ92-413) in PEX1-KO cells results in partial complementation, i.e., a significant decrease of number of pre-peroxisomal vesicles, however not completely reaching T-REx293 levels. This demonstrates that the structural requirements for PEX1 to perform protein import or abundance of peroxisomal vesicles is not identical: While the AAA$^+$-ATPase domains are essential for both functions, the N-terminal region is only required for recovery of peroxisomal matrix protein import. Therefore, it is suggestive that the novel 'moonlighting' function of PEX1, which leads to a reduction of the number of vesicles is at least partially independent from extraction of the import receptor from the peroxisomal membrane.

Discussion

Zellweger patient-derived cell lines were the only source for phenotype/genotype correlation of the human familiar diseases for decades (Ferdinandusse et al. 2016). However, differences in genetic or epigenetic background of patient derived cell lines and residual expression of mutated PEX genes hamper comparative studies. To minimize the effects of diversity and uncertainty, we generated selected PEX knockouts in isogenic T-REx293 cells, using the CRISPR/Cas9 technology. A potential drawback of such a cell line collection is that it does not reflect the tissue specific surrounding, and that the expression of the disease phenotype might depend on the individual exome of the patients, which is not reflected in the isogenic cells. However, the generated cell line collection allows a comparable dissection of the contribution of patient's mutations independent of individual influences. The deleted PEX genes in our study are either involved in *de novo* membrane synthesis (PEX3, PEX16 and PEX19) or represent key constituents of the receptor cycle for matrix protein import: PEX5 & PEX7 (signal recognition), PEX13 & PEX14

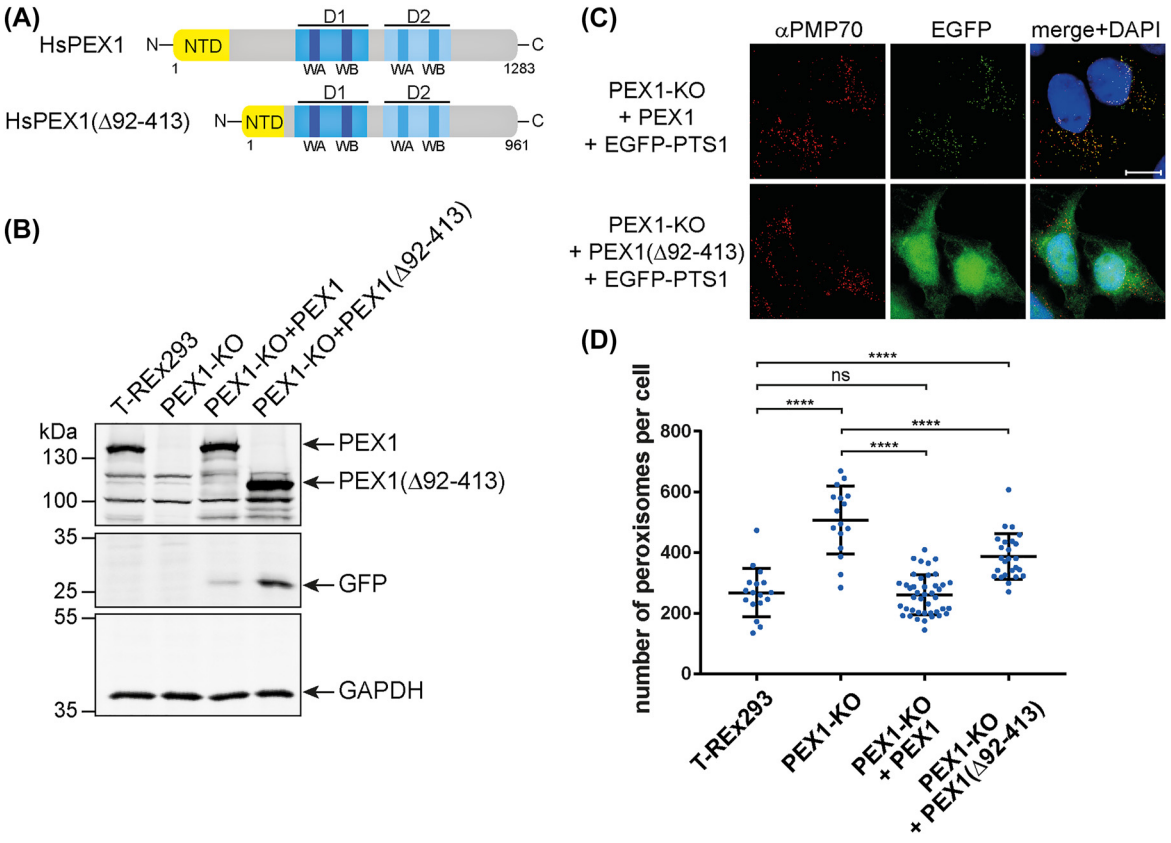

Figure 5: Functional analysis of an alternatively spliced PEX1 isoform. (A) Domain structure of the two known PEX1 isoforms. While both isoforms contain two AAA$^+$-ATPase domains (D1 and D2) with two Walker motifs (WA/WB) each, the short isoform of PEX1 lacks a stretch of 321 amino acids within the N-terminal regions (corresponding to amino acids 92–413 in the long isoform). (B) Adherent T-REx293, non-transfected PEX1-KO cells and PEX1-KO cells transfected with bicistronic plasmids encoding either PEX1 or PEX1(Δ92-413) were lysed in SDS-PAGE buffer and analyzed by immunoblotting using antibodies against PEX1, GFP and GAPDH. (C) To test the ability of both PEX1 isoforms to complement the import defect of matrix proteins, both were expressed in PEX1-KO cells in addition to the artificial matrix protein EGFP-PTS1 and analyzed by immunofluorescence microscopy. While the expression of PEX1 restored the import defect of peroxisomal matrix proteins, leading to the peroxisomal localization of EGFP-PTS1, the expression of PEX1(Δ92-413) could not complement the cytosolic mislocalization of EGFP-PTS1. Scale bar: 10 µm. (D) Influence of both PEX1 isoforms on peroxisomal numbers. Quantification was performed from whole cell images using the spots function of IMARIS (BITPLANE Scientific Software). Data represent mean ± SD. While the expression of PEX1 in PEX1-KO cells led to a complete reduction of peroxisomal numbers reaching T-REx293 levels, PEX1(Δ92-413) also significantly decreased the number of peroxisomal ghosts as analyzed by one-way ANOVA ($n \geq 2$, ****$p < 0.0001$, ns = not significant). Per replicate at least three cells were quantified for each cell line. Total number of cells analyzed: PEX1-KO + PEX1, 42; PEX1-KO + PEX1(Δ92-413), 25.

(receptor docking at the peroxisomal membrane), PEX10 & PEX1 (receptor ubiquitination and recycling).

For initial phenotypic analysis of the PEX-KO cell lines, peroxisome morphology and steady-state level of various peroxisomal membrane and matrix proteins were compared. The mutants of the import machinery for matrix proteins, i.e., PEX5-, PEX7-, PEX13-, PEX14-, PEX10- and PEX1-KO cells, are defective in matrix protein import but they contain peroxisomal membrane ghosts (Figure 2B). In accordance with the analysis of Zellweger patient-derived cell lines, no peroxisomes or empty membrane ghosts were detectable in PEX3-and PEX19-KO cells (Figure 2B). Remarkably, deletion of PEX16, which is also involved in the biogenesis of peroxisomal membrane proteins, revealed a heterogeneous phenotype (Figure 2B, Supplementary Figure S1). While in most PEX16-KO cells peroxisomal ghosts were completely absent, some cells harbor a few PMP70-labelled structures with a functional matrix protein import machinery. This is surprising since PEX16-defective fibroblasts from Zellweger patients are characterized by complete loss of peroxisomes (Honsho et al. 1998; Shaheen et al. 2011; Shimozawa et al. 2002). Very recently, Yagita et al. reported the same phenomenon of phenotypic mosaicism in different mammalian CRISPR/Cas9 generated PEX16-KO cell lines (Yagita et al. 2022). Therefore, it can be speculated that the complete loss of peroxisomes in Zellweger fibroblasts is specific for this cell type or forced by expression of deleterious PEX16

fragments. Nevertheless, the heterogenic phenotype of CRISPR/Cas9 generated KO cells demonstrates that PEX16 is involved but not always essential for *de novo* biogenesis of peroxisomes in human cells. Interestingly, this is in accordance with observations made in several yeasts, insect cells and plants (Burkhart et al. 2019; Eitzen et al. 1997; Farre et al. 2017; Nakayama et al. 2011; Opalinski et al. 2012). The non-essentiality of PEX16 could help to explain that in some model organisms, i.e., baker's yeast *Saccharomyces cerevisiae*, PEX16 homologues are not present (Smith and Aitchison 2013).

Our comparative analyses shows that mutants differ with respect to proteolytic cleavage of thiolase, which is performed by the peroxisomal PTS1-containing protease TYSND1 (Kurochkin et al. 2007). It is noteworthy that the limited proteolysis is greatly reduced in PEX3-and PEX19-KO cells. These cells are defective in peroxisomal membrane biogenesis and therefore lack peroxisomal membrane ghosts and all matrix enzymes reside in the cytosol. The lack of effective proteolytic cleavage of thiolase in these cells indicates that peroxisomal compartmentation of matrix enzymes is required for efficient processing of thiolase. The detection of matured thiolase in some of the mutants therefore comes as surprise and might be indicative for residual import into the peroxisomal ghosts in PEX13-, PEX14-, PEX10- and PEX1-KO cells lines (Figure 3), but this needs further investigation. The presence of cleaved thiolase, maybe as an indication for residual import, is especially pronounced for PEX10-KO cells, in which the direct comparison to other PEX-KO cells reveals an increased amount of processed thiolase (Figure 3). The observation that there is no cleavage product in PEX7-KO cells is explained by the fact that the PTS1-containing TYSND1 is still imported into peroxisomes with no access to the PTS2-containing thiolase that is mislocalized to the cytosol in the absence of the PTS2-receptor PEX7.

A striking novel feature of PEX1-deficient cells is the increased number of PMP70-labelled peroxisomal ghosts when compared with the other PEX-KO cells. The peroxisomal structures of PEX1-KO cells appeared to be smaller than the ghosts of other KO cells (Figure 2B). This phenotype of an increasing number of obviously smaller peroxisomal structures was complemented by expression of PEX1, demonstrating a specific effect of PEX1 on peroxisome homeostasis (Figures 2C, 4A). In contrast, patient-derived PEX1-deficient cells displayed a reduced number of peroxisomes when compared with normal fibroblasts (Chang et al. 1999). The reduced number of peroxisomes is in line with the well characterized role of the AAA^+-ATPases PEX1/PEX6 in extraction of the cycling import receptor PEX5 from the membrane. Defects in this dislocation result in an accumulation of ubiquitinated PEX5 at the membrane that triggers degradation of peroxisomes (Law et al. 2017).

The increase of peroxisomal precursors in PEX1-KO cells suggests that PEX1 has an additional function in peroxisome homeostasis that so far has not been seen in Zellweger patient derived cells. What could be the nature of this 'moonlighting' function of PEX1? One possible answer is that PEX1 is required for fusion of pre-peroxisomal vesicles as suggested earlier for *Yarrowia lipolytica* and other yeast species (Titorenko et al. 2000; Titorenko and Rachubinski 2000). Van der Zand et al. reported that in baker's yeast biochemically distinct vesicles derived from ER membranes fuse to form peroxisomes in a Pex1/Pex6 dependent manner (van der Zand et al. 2012). In mammalian cells, it was suggested that peroxisomes can arise from the fusion of ER- and mitochondria-derived pre-peroxisomal vesicles (Sugiura et al. 2017). If PEX1 would be required for fusion events, the PMP70-labelled structures could represent peroxisomal precursors, which are more abundant before fusion. The fusion hypothesis is further supported by the heterogeneous distribution of different membrane proteins, i.e. PMP70 and PEX14 among the population of peroxisomal vesicles in PEX1-KO cells (Figure 4A).

Computational mapping of the PEX1 exome revealed an alternatively spliced, short isoform in human cells, which was not characterized so far. Expression of this isoform, PEX1(Δ92-413), in PEX1-KO cells did not rescue the import defect for matrix proteins (Figure 5C) although both ATPase domains that are required for the interaction with PEX6 and receptor recycling are not affected (Schieferdecker and Wendler 2019). Thus, our data are clear in that the N-terminal region plays a critical role for matrix protein import. Along this line, it has been reported that the N-terminal domain of PEX1 contains a possible ubiquitin binding motif and might play a role in recognition of the ubiquitinated receptor for its export as part of the receptor cycle (Schwerter et al. 2018; Tan et al. 2016). However, expression of the short isoform did complement the PEX1-caused increase in peroxisomal ghosts (Figure 5D), demonstrating that the N-terminal fragment consisting of amino acids 92–402 is not essential for the moonlighting function in peroxisome homeostasis. Altogether, our data suggest that both PEX1 isoforms have separate functions in different states of peroxisome biogenesis. It will be interesting to investigate whether other peroxins also have isoforms with additional functions for which the generated PEX-KO cell lines could be of great benefit.

The generated resource of KO-cells is expected to serve as a valuable tool to elucidate the full spectrum of cellular functions of individual peroxins and their mutagenic and alternatively spliced isoforms. Here, the comparative

analyses of PEX-KO cells with isogenic background disclosed a moonlighting function of PEX1 in peroxisome homeostasis and PEX-KO-specific differences in thiolase processing.

Materials and methods

Plasmids

The generation of a bicistronic plasmid (pIRES2) for the expression of solely EGFP-PTS1 (C-terminal PTS1 sequence -SKL) or in combination with PEX5 and PEX14 was described elsewhere (Neuhaus et al. 2014). For the creation of a PEX19-containing complementation vector, pGEX-4T-1-PEX19 was digested with BamHI/SalI and inserted in BglII/SalI-digested pIRES2-EGFP-PEX14. PEX1 was PCR-amplified with the primer pair 5′-gatcgctagc atgtggggcagcgatcgcctgg-3′ and 5′-gatcggatccttatgctaaagttactttctgtccag-3′ and inserted into BamHI/BmtI digested pIRES2-EGFP-PTS1. For construction of complementation vectors, pIRES2-EGFP-PTS1 was PCR-amplified (5′-gtcgacggtaccgcggg-3′, 5′-gtgaaccgtcagatccgctagc-3′) and PCR-amplified PEX-genes were inserted by overhangs (PEX3: pM-PEX3, 5′-accgtcagatccgctagcatgctgaggtctgtatggaattttctgaaacgc-3′, 5′-gtacccctcagcaactggagaaatgagtcgacggtaccgcgggc-3′; PEX10: pM-PEX10, 5′-accgtcagatccgctagcatggccccggccgccg-3′, 5′-catctaccttcggcactaccgctgagtcgacggtaccgcgggc-3′; PEX13: pM-PEX13, 5′-accgtcagatccgctagcatggcgtcccagccgcca-3′, 5′-gcccgcggtaccgtcgactcaaagatcttgcttttctccatctttccca-3′; PEX16: pM-PEX16, 5′-accgtcagatccgctagcatggagaagctgcggctcctgg-3′, 5′-cagaaaatctacttctacagttggggctgagtcgacggtaccgcgggc-3′). To test for PTS2-import, PTS2-EGFP (N-terminal PTS2 sequence RLQVVLGHL-) was PCR-amplified (pEGFPN1-PTS2-EGFP, 5′-atgataatatggccacaaccatgcatcggctgcaggtagtg-3′, 5′-ggcatggacgagctgtacaagtaacggccgcgactctagatcat-3′) and inserted into pIRES2-EGFP-PTS1, which was also amplified by PCR using the primer pair 5′-cggccgcgactctagatcataatc-3′ and 5′-gaaaaacacgatgataatatggccacaacc-3′. The PEX7-containing complementation vector was generated by ligation of PCR-amplified PEX7 (pM-PEX7, 5′-accgtcagatccgctagcatgagtgcggtgtgcggtgg-3′, 5′-ccctgcttgtcttactattcctgcttgagtcgacggtaccgcgggc-3′) and pIRES2-PTS2-EGFP (5′-gtcgacggtaccgcggg-3′, 5′-gctagcggatctgacggttcac-3′). Plasmids for generation of PEX5-and PEX14-CRISPR-KOs have been described elsewhere (Galiani et al. 2022), while for the remaining KO cell lines the following sense oligonucleotides were annealed with the corresponding antisense part and inserted into the pX458 vector (Addgene 48,138, Dr. Feng Zhang) to act as guide RNAs: PEX1 (5′-agcgatgcgctggcgggtgc-3′), PEX3 (5′-atgatattgtcgtcgtgctt-3′), PEX7 (5′-cgcgatgccgtagtgctgcg-3′), PEX10 (5′-cgcggatcacctccgggggg-3′), PEX13 (5′-ctgggagacccgccgaattc-3′), PEX16 (5′-ggtgacgagtcacgtactcc-3′), PEX19 (5′-ggggccccagaagagatcgcc-3′).

Cell culture

HEK T-REx293 cells were cultivated in Dulbecco's Modified Eagle's Medium high glucose (DMEM), supplemented with 10% fetal calf serum, 4 mM L-glutamine, 100,000 U/L penicillin and 100 mg/L streptomycin at 37 °C and 8.5% CO_2.

Transfections were done by using X-tremeGENE HP DNA Transfection Reagent (Roche, Germany) according to the manufacturer's instructions.

Generation of knockout cell lines using the CRISPR/Cas9 system

For the generation of T-REx293 PEX1-, PEX3-, PEX7-, PEX10-, PEX13-, PEX16-and PEX19-KO cell lines, T-REx293 cells were transfected with specific CRISPR-vectors, containing the Cas9 endonuclease, the respective guide-sequence and EGFP. 48 h after transfection, EGFP-positive cells were sorted by fluorescence-activated cell sorting (FACS) in 96-well plates, containing DMEM, supplemented with additional 10% FCS. After expansion, several clones of each deletion cell line were seeded on coverslips and tested for the import of EGFP-PTS1/PTS2-EGFP or the presence of peroxisomal membranes by fluorescence microscopy. From clones showing an import defect or absence of peroxisomal membranes genomic DNA was isolated using the kit NucleoSpin Tissue (Macherey-Nagel), according to the manufacturer's instructions. The exon with expected double strand break was then PCR-amplified using the Terra PCR Direct Polymerase Mix (Takara) and compared to the wild-type sequence by the TIDE algorithm (Brinkman et al. 2014). The amplified exons of clones that showed base pair insertions or deletions on every allele resulting in a frame shift were inserted in pGEM-T, amplified and sequenced to obtain the remaining expression products. The generation of the T-REx293 PEX5-and PEX14-KO cell lines has been described elsewhere (Galiani et al. 2022).

Preparation of whole cell lysates and immunoblot analysis

For the preparation of whole cell lysates, cells were seeded to >90% confluence on 6 cm plates. Cells were washed with Hanks' Balanced Salt Solution (HBSS) without $MgCl_2$, trypsinized and resuspended in HBSS+$MgCl_2$. Cells were harvested (2000 rpm, 7 min, 4 °C) and resuspended in RIPA buffer (150 mM NaCl, 1% (v/v) IGEPAL, 0.5% (w/v) sodium deoxycholate, 0.1% (w/v) SDS, 50 mM Tris pH 8, cOmplete™ EDTA-free Protease Inhibitor Cocktail (Roche), 25 µg/mL DNase). After 30 min on ice cell debris was sedimented (13,000 rpm, 5 min, 4 °C) and SDS-sample buffer was added to the supernatant. Alternatively, adherent cells were directly lysed in SDS-PAGE sample buffer. Samples were analyzed by SDS-PAGE and immunoblotting using the following antibodies: rabbit *α*PEX1 (1:1,000, Proteintech), rabbit *α*PEX5 (1:5,000, (Fodor et al. 2015)), rabbit *α*PEX13 (1:1,000, Proteintech), rabbit *α*PEX14 (1:5,000, (Will et al. 1999)), rabbit *α*PEX19 (1:5,000, Thermo Fisher Scientific), rabbit *α*ACAA1 (1:1,000, Sigma-Aldrich), mouse *α*GFP (1:2,000, Proteintech) and mouse *α*GAPDH (1:7,500, Proteintech). As secondary antibodies IRDye 800CW goat *α*rabbit and IRDye 800CW goat *α*mouse (1:15,000, LI-COR, Lincoln (USA)) were used.

Fluorescence microscopy

For fluorescence microscopy, cells were seeded on coverslips to an appropriate density, washed with D'PBS and fixed using 3% formaldehyde for 20 min. Afterwards, membranes were permeabilized in 1% Triton X-100 for 5 min and free binding sites were blocked with 2% BSA for 1 h. Next, cells were incubated for 30 min with the primary antibodies, rabbit *α*PMP70 (1:500, Invitrogen) and chicken *α*PEX14 (1:500, Ruhr-University Bochum), and afterwards with the secondary

antibodies goat α-rabbit IgG (H+L) Alexa Fluor 594 (Invitrogen) and goat α-chicken IgG (H+L) Alexa Fluor 647 (Invitrogen). Coverslips were mounted on glass slides using Mowiol 4–88 (Calbiochem), supplemented with DAPI. Imaging was performed using the Zeiss ELYRA PS.1 Super-Resolution Structured Illumination Microscope (SR-SIM, Zeiss). All images were taken in one focal plane. Peroxisomal quantification was performed by applying the spots-function of IMARIS (BITPLANE Scientific Software) on microscopic whole-cell images.

Statistical analysis

Statistical analysis was performed by one-way ANOVA with Tukey's multiple comparisons using GraphPad Prism (Graphpad Software, Inc, USA). Data were considered significant at a value of $*p < 0.05$.

Acknowledgments: We thank Meike Jade, Cristina Pintado and Bernhild Erdmann for their support.
Author contributions: All the authors have accepted responsibility for the entire content of this submitted manuscript and approved submission.
Research funding: This work was supported by the Deutsche Forschungsgemeinschaft (FOR1905, ER178/6-2, ER178/7-2). https://gepris.dfg.de/gepris/projekt/219314758.
Conflict of interest statement: The authors declare no conflicts of interest regarding this article.

References

Binz, R.L., Tian, E., Sadhukhan, R., Zhou, D., Hauer-Jensen, M., and Pathak, R. (2019). Identification of novel breakpoints for locus- and region-specific translocations in 293 cells by molecular cytogenetics before and after irradiation. Sci. Rep. 9: 10554.

Bowen, P., Lee, C.S., Zellweger, H., and Lindenberg, R. (1964). A familial syndrome of multiple congenital defects. Bull. Johns Hopkins Hosp. 114: 402–414.

Brinkman, E.K., Chen, T., Amendola, M., and Van Steensel, B. (2014). Easy quantitative assessment of genome editing by sequence trace decomposition. Nucleic Acids Res. 42: e168.

Burkhart, S.E., Llinas, R.J., and Bartel, B. (2019). PEX16 contributions to peroxisome import and metabolism revealed by viable *Arabidopsis* pex16 mutants. J. Integr. Plant Biol. 61: 853–870.

Chang, C.C., South, S., Warren, D., Jones, J., Moser, A.B., Moser, H.W., and Gould, S.J. (1999). Metabolic control of peroxisome abundance. J. Cell Sci. 112: 1579–1590.

Chen, X., Devarajan, S., Danda, N., and Williams, C. (2018). Insights into the role of the peroxisomal ubiquitination machinery in Pex13p degradation in the yeast *Hansenula polymorpha*. J. Mol. Biol. 430: 1545–1558.

Ciniawsky, S., Grimm, I., Saffian, D., Girzalsky, W., Erdmann, R., and Wendler, P. (2015). Molecular snapshots of the Pex1/6 AAA+ complex in action. Nat. Commun. 6: 7331.

Dodt, G. and Gould, S.J. (1996). Multiple *PEX* genes are required for proper subcellular distribution and stability of Pex5p, the PTS1 receptor: evidence that PTS1 protein import is mediated by a cycling receptor. J. Cell Biol. 135: 1763–1774.

Doudna, J.A. and Charpentier, E. (2014). Genome editing. The new frontier of genome engineering with CRISPR-Cas9. Science 346: 1258096.

Ebberink, M.S., Mooijer, P.A., Gootjes, J., Koster, J., Wanders, R.J., and Waterham, H.R. (2011). Genetic classification and mutational spectrum of more than 600 patients with a zellweger syndrome spectrum disorder. Hum. Mutat. 32: 59–69.

Eitzen, G.A., Szilard, R.K., and Rachubinski, R.A. (1997). Enlarged peroxisomes are present in oleic acid-grown *Yarrowia lipolytica* overexpressing the PEX16 gene encoding an intraperoxisomal peripheral membrane peroxin. J. Cell Biol. 137: 1265–1278.

Farre, J.C., Carolino, K., Stasyk, O.V., Stasyk, O.G., Hodzic, Z., Agrawal, G., Till, A., Proietto, M., Cregg, J., Sibirny, A.A., et al. (2017). A new yeast peroxin, Pex36, a functional homolog of mammalian PEX16, functions in the ER-to-peroxisome traffic of peroxisomal membrane proteins. J. Mol. Biol. 429: 3743–3762.

Ferdinandusse, S., Ebberink, M.S., Vaz, F.M., Waterham, H.R., and Wanders, R.J. (2016). The important role of biochemical and functional studies in the diagnostics of peroxisomal disorders. J. Inherit. Metab. Dis. 39: 531–543.

Fodor, K., Wolf, J., Reglinski, K., Passon, D.M., Lou, Y., Schliebs, W., Erdmann, R., and Wilmanns, M. (2015). Ligand-induced compaction of the PEX5 receptor-binding cavity impacts protein import efficiency into peroxisomes. Traffic 16: 85–98.

Fransen, M., Terlecky, S.R., and Subramani, S. (1998). Identification of a human PTS1 receptor docking protein directly required for peroxisomal protein import. Proc. Natl. Acad. Sci. U.S.A. 95: 8087–8092.

Galiani, S., Reglinski, K., Carravilla, P., Barbotin, A., Urbančič, I., Ott, J., Sehr, J., Sezgin, E., Schneider, F., Waithe, D., et al. (2022). Diffusion and interaction dynamics of the cytosolic peroxisomal import receptor PEX5. Biophys. Rep. 2: 100055.

Goldfischer, S., Moor, C.L., Johnson, A.B., Spiro, A.J., Valsamis, M.P., Wisniewski, H.K., Ritch, R.H., Norton, W.T., Rapin, I., and Gerner, L.M. (1973). Peroxisomal and mitochondrial defects in cerebrohepatorenal syndrome. Science 182: 62–64.

Gould, S.J., Kalish, J.E., Morrell, J.C., Bjorkman, J., Urquhart, A.J., and Crane, D.I. (1996). Pex13p is an SH3 protein of the peroxisome membrane and a docking factor for the predominantly cytoplasmic PTs1 receptor. J. Cell Biol. 135: 85–95.

Gould, S.J., Keller, G.A., Hosken, N., Wilkinson, J., and Subramani, S. (1989). A conserved tripeptide sorts proteins to peroxisomes. J. Cell Biol. 108: 1657–1664.

Grou, C.P., Francisco, T., Rodrigues, T.A., Freitas, M.O., Pinto, M.P., Carvalho, A.F., Domingues, P., Wood, S.A., Rodriguez-Borges, J.E., Sa-Miranda, C., et al. (2012). Identification of ubiquitin-specific protease 9X (USP9X) as a deubiquitinase acting on ubiquitin-peroxin 5 (PEX5) thioester conjugate. J. Biol. Chem. 287: 12815–12827.

Honsho, M., Tamura, S., Shimozawa, N., Suzuki, Y., Kondo, N., and Fujiki, Y. (1998). Mutation in *PEX16* is causal in the peroxisome-deficient zellweger syndrome of complementation group D. Am. J. Hum. Genet. 63: 1622–1630.

Jinek, M., Chylinski, K., Fonfara, I., Hauer, M., Doudna, J.A., and Charpentier, E. (2012). A programmable dual-RNA-guided DNA endonuclease in adaptive bacterial immunity. Science 337: 816–821.

Kurochkin, I.V., Mizuno, Y., Konagaya, A., Sakaki, Y., Schonbach, C., and Okazaki, Y. (2007). Novel peroxisomal protease Tysnd1 processes PTS1-and PTS2-containing enzymes involved in β-oxidation of fatty acids. EMBO J. 26: 835–845.

Law, K.B., Bronte-Tinkew, D., Pietro, E.D., Snowden, A., Jones, R.O., Moser, A., Brumell, J.H., Braverman, N., and Kim, P.K. (2017). The peroxisomal AAA ATPase complex prevents pexophagy and development of peroxisome biogenesis disorders. Autophagy 13: 868–884.

Matsumoto, N., Tamura, S., Furuki, S., Miyata, N., Moser, A., Shimozawa, N., Moser, H.W., Suzuki, Y., Kondo, N., and Fujiki, Y. (2003). Mutations in novel peroxin gene PEX26 that cause peroxisome-biogenesis disorders of complementation group 8 provide a genotype-phenotype correlation. Am. J. Hum. Genet. 73: 233–246.

Matsumoto, N., Tamura, S., Moser, A., Moser, H.W., Braverman, N., Suzuki, Y., Shimozawa, N., Kondo, N., and Fujiki, Y. (2001). The peroxin Pex6p gene is impaired in peroxisomal biogenesis disorders of complementation group 6. J. Hum. Genet. 46: 273–277.

Meinecke, M., Cizmowski, C., Schliebs, W., Kruger, V., Beck, S., Wagner, R., and Erdmann, R. (2010). The peroxisomal importomer constitutes a large and highly dynamic pore. Nat. Cell Biol. 12: 273–277.

Miyata, N. and Fujiki, Y. (2005). Shuttling mechanism of peroxisome targeting signal type 1 receptor Pex5: ATP-independent import and ATP-dependent export. Mol. Cell Biol. 25: 10822–10832.

Moser, A.B., Rasmussen, M., Naidu, S., Watkins, P.A., Mcguinness, M., Hajra, A.K., Chen, G., Raymond, G., Liu, A., Gordon, D., et al. (1995). Phenotype of patients with peroxisomal disorders subdivided into sixteen complementation groups. J. Pediatr. 127: 13–22.

Nakayama, M., Sato, H., Okuda, T., Fujisawa, N., Kono, N., Arai, H., Suzuki, E., Umeda, M., Ishikawa, H.O., and Matsuno, K. (2011). Drosophila carrying pex3 or pex16 mutations are models of Zellweger syndrome that reflect its symptoms associated with the absence of peroxisomes. PLoS One 6: e22984.

Natsuyama, R., Okumoto, K., and Fujiki, Y. (2013). Pex5p stabilizes Pex14p: a study using a newly isolated pex5 CHO cell mutant, ZPEG101. Biochem. J. 449: 195–207.

Neuhaus, A., Kooshapur, H., Wolf, J., Meyer, N.H., Madl, T., Saidowsky, J., Hambruch, E., Lazam, A., Jung, M., Sattler, M., et al. (2014). A novel Pex14 protein-interacting site of human Pex5 is critical for matrix protein import into peroxisomes. J. Biol. Chem. 289: 437–448.

Nuebel, E., Morgan, J.T., Fogarty, S., Winter, J.M., Lettlova, S., Berg, J.A., Chen, Y.C., Kidwell, C.U., Maschek, J.A., Clowers, K.J., et al. (2021). The biochemical basis of mitochondrial dysfunction in Zellweger spectrum disorder. EMBO Rep. 22: e51991.

Opalinski, L., Bartoszewska, M., Fekken, S., Liu, H., De Boer, R., Van Der Klei, I., Veenhuis, M., and Kiel, J.A. (2012). De novo peroxisome biogenesis in Penicillium chrysogenum is not dependent on the Pex11 family members or Pex16. PLoS One 7: e35490.

Osumi, T., Tsukamoto, T., Hata, S., Yokota, S., Miura, S., Fujiki, Y., Hijikata, M., Miyazawa, S., and Hashimoto, T. (1991). Amino-terminal presequence of the precursor of peroxisomal 3-ketoacyl-CoA thiolase is a cleavable signal peptide for peroxisomal targeting. Biochem. Biophys. Res. Commun. 181: 947–954.

Otera, H., Harano, T., Honsho, M., Ghaedi, K., Mukai, S., Tanaka, A., Kawai, A., Shimizu, N., and Fujiki, Y. (2000). The mammalian peroxin Pex5pL, the longer isoform of the mobile peroxisome targeting signal (PTS) type 1 transporter, translocates the Pex7p.PTS2 protein complex into peroxisomes via its initial docking site, Pex14p. J. Biol. Chem. 275: 21703–21714.

Portsteffen, H., Beyer, A., Becker, E., Epplen, C., Pawlak, A., Kunau, W.H., and Dodt, G. (1997). Human PEX1 is mutated in complementation group 1 of the peroxisome biogenesis disorders. Nat. Genet. 17: 449–452.

Sacksteder, K.A., Jones, J.M., South, S.T., Li, X., Liu, Y., and Gould, S.J. (2000). PEX19 binds multiple peroxisomal membrane proteins, is predominantly cytoplasmic, and is required for peroxisome membrane synthesis. J. Cell Biol. 148: 931–944.

Saffert, P., Enenkel, C., and Wendler, P. (2017). Structure and function of p97 and Pex1/6 type II AAA+ complexes. Front. Mol. Biosci. 4: 33.

Santos, M.J., Imanaka, T., Shio, H., Small, G.M., and Lazarow, P.B. (1988). Peroxisomal membrane ghosts in Zellweger syndrome-aberrant organelle assembly. Science 239: 1536–1538.

Schieferdecker, A. and Wendler, P. (2019). Structural mapping of missense mutations in the Pex1/Pex6 complex. Int. J. Mol. Sci. 20: 3756.

Schwerter, D., Grimm, I., Girzalsky, W., and Erdmann, R. (2018). Receptor recognition by the peroxisomal AAA complex depends on the presence of the ubiquitin moiety and is mediated by Pex1p. J. Biol. Chem. 293: 15458–15470.

Shaheen, R., Al-Dirbashi, O.Y., Al-Hassnan, Z.N., Al-Owain, M., Makhsheed, N., Basheeri, F., Seidahmed, M.Z., Salih, M.A., Faqih, E., Zaidan, H., et al. (2011). Clinical, biochemical and molecular characterization of peroxisomal diseases in Arabs. Clin. Genet. 79: 60–70.

Shimozawa, N., Nagase, T., Takemoto, Y., Suzuki, Y., Fujiki, Y., Wanders, R.J., and Kondo, N. (2002). A novel aberrant splicing mutation of the PEX16 gene in two patients with Zellweger syndrome. Biochem. Biophys. Res. Commun. 292: 109–112.

Shimozawa, N., Suzuki, Y., Zhang, Z., Imamura, A., Ghaedi, K., Fujiki, Y., and Kondo, N. (2000). Identification of PEX3 as the gene mutated in a Zellweger syndrome patient lacking peroxisomal remnant structures. Hum. Mol. Genet. 9: 1995–1999.

Shiozawa, K., Goda, N., Shimizu, T., Mizuguchi, K., Kondo, N., Shimozawa, N., Shirakawa, M., and Hiroaki, H. (2006). The common phospholipid-binding activity of the N-terminal domains of PEX1 and VCP/p97. FEBS J. 273: 4959–4971.

Slawecki, M.L., Dodt, G., Steinberg, S., Moser, A.B., Moser, H.W., and Gould, S.J. (1995). Identification of three distinct peroxisomal protein import defects in patients with peroxisome biogenesis disorders. J. Cell Sci. 108: 1817–1829.

Smith, J.J. and Aitchison, J.D. (2013). Peroxisomes take shape. Nat. Rev. Mol. Cell Biol. 14: 803–817.

South, S.T. and Gould, S.J. (1999). Peroxisome synthesis in the absence of preexisting peroxisomes. J. Cell Biol. 144: 255–266.

Subramani, S. (1998). Components involved in peroxisome import, biogenesis, proliferation, turnover, and movement. Physiol. Rev. 78: 171–188.

Sugiura, A., Mattie, S., Prudent, J., and Mcbride, H.M. (2017). Newly born peroxisomes are a hybrid of mitochondrial and ER-derived pre-peroxisomes. Nature 542: 251–254.

Suzuki, Y., Shimozawa, N., Imamura, A., Fukuda, S., Zhang, Z., Orii, T., and Kondo, N. (2001). Clinical, biochemical and genetic aspects and neuronal migration in peroxisome biogenesis disorders. J. Inherit. Metab. Dis. 24: 151–165.

Tan, D., Blok, N.B., Rapoport, T.A., and Walz, T. (2016). Structures of the double-ring AAA ATPase Pex1-Pex6 involved in peroxisome biogenesis. FEBS J. 283: 986–992.

Titorenko, V.I., Chan, H., and Rachubinski, R.A. (2000). Fusion of small peroxisomal vesicles *in vitro* reconstructs an early step in the *in vivo* multistep peroxisome assembly pathway of *Yarrowia lipolytica*. J. Cell Biol. 148: 29–44.

Titorenko, V.I. and Rachubinski, R.A. (2000). Peroxisomal membrane fusion requires two AAA family ATPases, Pex1p and Pex6p. J. Cell Biol. 150: 881–886.

Van Der Zand, A., Gent, J., Braakman, I., and Tabak, H.F. (2012). Biochemically distinct vesicles from the endoplasmic reticulum fuse to form peroxisomes. Cell 149: 397–409.

Will, G.K., Soukupova, M., Hong, X., Erdmann, K.S., Kiel, J.A., Dodt, G., Kunau, W.H., and Erdmann, R. (1999). Identification and characterization of the human orthologue of yeast Pex14p. Mol. Cell Biol. 19: 2265–2277.

Yagita, Y., Abe, Y., and Fujiki, Y. (2022). *De novo* formation and maintenance of mammalian peroxisomes in the absence of PEX16. J. Cell Sci 135: jcs258377.

Supplementary Material: This article contains supplementary material (https://doi.org/10.1515/hsz-2022-0223).